AJNR Am J Neuroradiol 22:248–254, February 2001

Measurement of Cerebral Hemodynamics with Perfusion-weighted MR Imaging: Comparison with Pre- and Post-acetazolamide ^{133}Xe-SPECT in Occlusive Carotid Disease

Keiichi Kikuchi, Kenya Murase, Hitoshi Miki, Takanori Kikuchi, Yoshifumi Sugawara, Teruhito Mochizuki, Junpei Ikezoe, and Shiro Ohue

BACKGROUND AND PURPOSE: **We generated regional cerebral blood volume (rCBV) and regional cerebral blood flow (rCBF) studies from dynamic susceptibility contrast-enhanced MR images after an intravenous bolus injection of contrast agent (perfusion-weighted imaging [PWI]) by applying indicator dilution theory. We used a multishot echo-planar imaging (EPI) sequence to obtain adequate arterial input function (AIF). Our purpose was to compare the cerebral hemodynamics measured by PWI with the rCBF values and cerebral perfusion reserve obtained by xenon-133 single-photon emission CT (^{133}Xe-SPECT).**

METHODS: **Eight patients with chronic internal carotid artery occlusion or stenosis were examined. PWI data were acquired using a multishot EPI sequence, and the AIF was determined automatically. Our procedure was based on indicator dilution theory and deconvolution analysis. To eliminate the effect of superficial vessels, the automatic threshold selection method was used.**

RESULTS: **AIF was adequate to generate rCBF and rCBV images. The rCBF and rCBV images by PWI were superior to ^{133}Xe-SPECT scans in spatial resolution, and the rCBF values obtained by PWI correlated well with those obtained by ^{133}Xe-SPECT. The regions with severely decreased perfusion reserve, which were determined by pre- and post-acetazolamide ^{133}Xe-SPECT, showed significantly lower rCBF and higher rCBV by PWI than did regions with normal and moderately decreased perfusion reserve.**

CONCLUSION: **The rCBF and rCBV images generated by our procedure using PWI data appear to provide important clinical information for evaluating the degree of cerebral perfusion reserve impairment in patients with chronic ischemia.**

Absolute regional cerebral blood volume (rCBV) and regional cerebral blood flow (rCBF) are important parameters for determining the management of patients with ischemic cerebrovascular disease (1–5). rCBV and rCBF values have been measured by positron emission tomography (PET) using labeled carbon monoxide or O-15 H_2O (6, 7) and by single-photon emission CT (SPECT) using xenon-133 (8), N-isopropyl-p-(I-123)iodoamphetamine (9), ^{99m}Tc-hexamethylpropyleneamine oxime (10), or ^{99m}Tc-ethyl cysteinate dimer (11). PET can accurately portray rCBF or rCBV with reasonable resolution; however, PET is not widely used in the clinical setting because of its high cost and limited availability. Therefore, despite its relatively poor resolution, SPECT has been used to assess rCBF and rCBF reserve to help determine surgical indications in the clinical setting (12–14).

Conventional MR imaging techniques (T1-weighted, T2-weighted, and fluid-attenuated inversion recovery sequences) provide high-resolution and high-contrast anatomic information in patients with ischemic cerebrovascular disease. Perfusion-weighted imaging (PWI) (15–17), dynamic susceptibility contrast MR imaging after a bolus injection of intravascular contrast agent, has been used to calculate rCBV and rCBF. Recently, the clinical usefulness of PWI for depicting acute cerebral infarction has also been reported (18–20). Quantification of rCBF and rCBV can be done with PWI (referred to as rCBF-PWI and rCBV-PWI, respec-

T.K., Y.S., T.M., J.I.) and Neurological Surgery (S.O.), Ehime University School of Medicine, Ehime, Japan.

Address reprint requests to Keiichi Kikuchi, MD, Department of Radiology, Ehime University School of Medicine, Shitsukawa, Shigenobu-cho, Onsen-gun, Ehime, 791-0295 Japan.

Data for eight patients with occlusive carotid disease

Patient No.	Age (y)/Sex	Symptoms	Diagnosis	Side on which Arterial Input Function Was Obtained
1	66/M	Free	R ICA stenosis	L
2	58/M	TIA	R ICA occlusion	L
3	69/M	Free	L ICA occlusion, R ICA stenosis	R
4	64/M	Free	R ICA stenosis	L
5	64/M	L hemiparesis	R ICA occlusion	L
6	61/M	TIA	R ICA occlusion, L ICA stenosis	L
7	55/M	Free	L ICA stenosis	R
8	68/F	Free	R ICA occlusion, L ICA stenosis	L

Note.—TIA indicates transient ischemic attack; ICA, internal carotid artery.

tively) by applying indicator dilution theory (21–26). However, to assess rCBF and rCBV, indicator dilution theory requires arterial concentration of the contrast agent as an arterial input function (AIF), which is a demanding and complicated process in the clinical setting. In this study, we used a multishot gradient-echo type echo-planar imaging (EPI) sequence for PWI, and the AIF was obtained automatically from the internal carotid artery (ICA). The generated rCBF and rCBV images using PWI data were compared with rCBF and with the percentage of CBF increase (% increase) after acetazolamide load using ^{133}Xe-SPECT in patients with chronic ischemia and occlusive carotid disease.

Methods

Subjects

Eight patients (seven men and one woman, 55 to 69 years old; mean age, 63 years) with chronic ICA occlusion or stenosis were included in the study (Table). All patients underwent PWI and ^{133}Xe-SPECT before and after acetazolamide administration within 1 month for preoperative evaluation of extracranial-intracranial (EC-IC) bypass surgery or carotid endarterectomy. Occlusive lesions of the ICA were confirmed by digital subtraction angiography in seven patients and by CT angiography in one patient.

Written informed consent was obtained from all patients after detailed explanation of the purpose of the study and scanning procedure.

Perfusion MR Imaging Protocol

PWI studies were performed on a 1.5-T MR unit using a multishot gradient-echo type EPI pulse sequence with parameters of 255–319/30 (TR/TE), a 35° to 40° flip angle, and an echo factor of 9. The acquisition matrix was 128 × 60 with a field of view of 23 × 17 cm, and the slice thickness was 6 mm. A 10-mL bolus of gadopentetate dimeglumine was injected through an antecubital vein with a 22-gauge cannula at a speed of 3 mL/s by an MR-compatible power injector, followed by 20 mL of saline. Forty to fifty dynamic images, covering four to six slices, were then obtained at a speed of 1.32 to 2.08 seconds. One slice included the cavernous portion of the ICA for obtaining the AIF, and other slices covered the cerebrum parallel to the anterior commissure-posterior commissure line.

Quantification of CBF and CBV

All PWI data were transferred to a postprocessing workstation, and quantitative rCBF-PWI and rCBV-PWI images were generated on a workstation using our proprietary software. The AIF was obtained automatically from the ICA contralateral to the occluded or severely stenosed ICA by fuzzy clustering (27).

In the first step, local changes in signal intensity during the bolus passage were computed pixel by pixel. For reduction of statistical noise, time-smoothing was performed using an averaging filter with a weight of [0.25, 0.5, 0.25]. The resulting signal-time curves were converted into concentration-time curves, assuming an exponential relationship between the relative signal reduction of $S(t)/S_0$ and local concentration of contrast agent C(t):

$$C(t) = \frac{-k}{TE} \cdot \ln\left(\frac{S(t)}{S_0}\right), \quad (1)$$

where S_0 denotes precontrast signal intensity; S(t) is the signal intensity at time, t, after injection of contrast agent; k is the tissue and field strength specific constant, and TE is the echo time (15).

According to the indicator dilution theory for intravascular contrast agent, when the AIF of the contrast agent entering the volume of interest (VOI) is known, CBF is implicitly given by

$$k_h C_{VOI}(t) = CBF \int_0^t C_{AIF}(\tau) \cdot R(t - \tau)\, d\tau \quad (2)$$

where $C_{VOI}(t)$ and $C_{AIF}(\tau)$ are the time-dependent concentrations of contrast agent in the VOI and the AIF, respectively. The constant k_h [$= (1-H_{LV})/(1-H_{SV})$] is a correction constant for the difference in hematocrit of the large (H_{LV}, approximately 0.45) and small (H_{SV}, approximately 0.25) blood vessels of the brain. R(t) is the residue function, which is the relative amount of contrast agent in the VOI in an idealized perfusion experiment, in which a unit area bolus is instantaneously injected [$R(0) = 1$] and subsequently washed out [$R(\infty) = 0$] by the perfusion. It is known from Equation 2 that the initial height of the deconvoluted time-concentration curve, that is, the tissue impulse response function h(t) [= CBF × R(t)] equals the CBF.

There are various approaches for calculating h(t) from Equation 2 by deconvolution. In this study, we adopted an algebraic approach based on singular value decomposition, which is robust against statistical noise. This approach was described in detail by Ostergaard et al (24). We generated the rCBF-PWI images by applying this approach pixel by pixel as follows:

$$CBF = K \cdot h(0), \quad (3)$$

where h(0) is the initial height of h(t) and K is a constant. The rCBV-PWI images were generated from

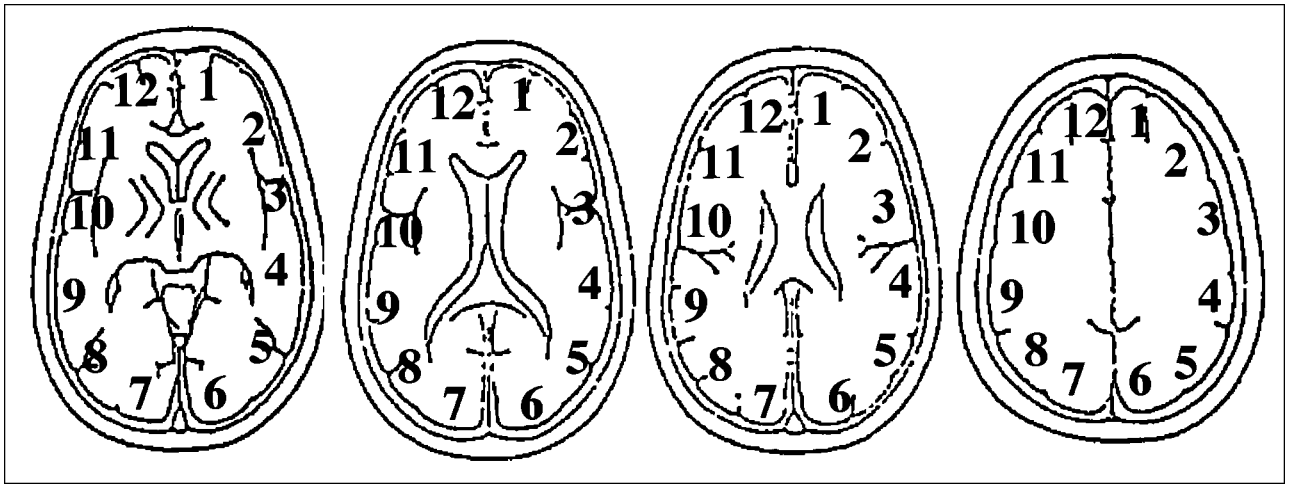

FIG 1. ROIs used for the analysis of cerebral perfusion. ROIs were placed on six regions in the brain parenchyma of each hemisphere. The ROIs were obtained from four slices on ^{133}Xe-SPECT scans and from two to four slices from PWI images. ROI 1 corresponded to the left ACA territory, ROI 2 to the left ABZ territory, ROIs 3 and 4 to the left MCA territory, ROI 5 to the left PBZ territory, and ROI 6 to the left PCA territory. ROIs 7 through 12 corresponded to the same territories in the right hemisphere. The ROI setting was consistent between ^{133}Xe-SPECT and PWI. Data from 10 regions were obtained for each patient.

$$rCBV = K \cdot \frac{\int_0^\infty C_{VOI}(\tau)\, d\tau}{\int_0^\infty C_{AIF}(\tau)\, d\tau}. \quad (4)$$

The K value in Equations 3 and 4 was determined by substituting 22 mL/100 g per minute for the CBF value of the white matter of the nonocclusive side (6, 7).

Because the superficial veins were prominent in the rCBF-PWI and rCBV-PWI images owing to the fact that the gradient-echo images were sensitive to the presence of large vessels (28, 29), we eliminated superficial vessels by using the automatic threshold selection method. First, we generated the gray-level histograms of the above images and considered two classes, classes 1 and 2, which were the pixels with and without superficial vessels, respectively. The optimal threshold value for discriminating these two classes was determined such that the following discriminant criterion measure, λ, was maximized:

$$\lambda = \frac{\sigma_B^2}{\sigma_W^2}, \quad (5)$$

where σ_W^2 and σ_B^2 are given by

$$\sigma_W^2 = P_1\sigma_1^2 + P_2\sigma_2^2 \quad \text{and} \quad \sigma_B^2 = P_1P_2(\mu_1 - \mu_2)^2,$$

respectively. P_1, P_2, μ_1, μ_2, σ_1, and σ_2 denote the probability of occurrence in class 1, the probability of occurrence in class 2, the class mean level in class 1, the class mean level in class 2, the class variance in class 1, and the class variance in class 2, respectively (30).

SPECT Protocol

^{133}Xe-SPECT was performed with a SPECT 2000H scanner. Patients inhaled 1.85 to 3.7 GBq of xenon-133 gas and CBF was measured according to the Kanno-Lassen method using dynamic SPECT data (16 scans with a duration of 20 seconds each) (31). The arterial input curve of xenon-133 was estimated from the end-expiratory xenon-133 concentration curve observed by a single NaI detector. The rCBF measurement by SPECT (rCBF-SPECT) was performed at rest (pre-rCBF); then, 15 minutes after intravenous administration of 1 g acetazolamide, a post-acetazolamide rCBF study (post-rCBF) was performed in the same manner (14). Cerebral perfusion reserve was evaluated by the % increase of CBF after acetazolamide as follows: % increase = [(post-rCBF) − (pre-rCBF)]/(pre-rCBF) × 100.

Data Analysis

We analyzed four tomographic planes of the basal ganglia through the centrum semiovale on ^{133}Xe-SPECT scans. On each imaging plane, regions of interest (ROIs) were placed on the cerebral cortex corresponding approximately to the territory of the anterior cerebral artery (ACA), anterior border zone (ABZ), middle cerebral artery (MCA), posterior border zone (PBZ), and posterior cerebral artery (PCA) of each hemisphere (Fig 1). On rCBF- and rCBV-PWI, ROIs were obtained from two to four slices, corresponding to Figure 1, for each patient. Mean CBF and CBV values in the ACA, ABZ, MCA, PBZ, and PCA were calculated from the corresponding ROIs in each hemisphere. The ROI setting was consistent between ^{133}Xe-SPECT and PWI. In all, 80 regions in eight patients were obtained, and two regions of complete infarction were excluded. Thus, 78 regions were analyzed in the current study.

The relationship between rCBF-PWI and rCBF-SPECT was evaluated using linear regression analysis. We classified the degree of perfusion reserve into three grades by the value of % increase (32): severely decreased perfusion reserve (% increase $\leq$ 0%; n = 10), moderately decreased perfusion reserve (0 $<$ % increase $\leq$ 15%; n = 16), and normal perfusion reserve (15% $<$ % increase; n = 52). The rCBF-SPECT, rCBF-PWI, and rCBV-PWI findings for the three groups of perfusion reserve were compared by means of analysis of variance followed by the Mann-Whitney *U*-test. A *P* value of less than .05 was considered significant.

Results

Adequate AIF was obtained from the ICA to generate rCBF-PWI and rCBV-PWI studies for all patients, regardless of the existence of occlusive carotid disease. Figure 2A shows a comparison of the AIFs obtained from the ICA and MCA in patient 7 (see Table). Note that their shapes vary slightly, and that the AIF obtained from the ICA was somewhat better than that from the MCA. Fig-

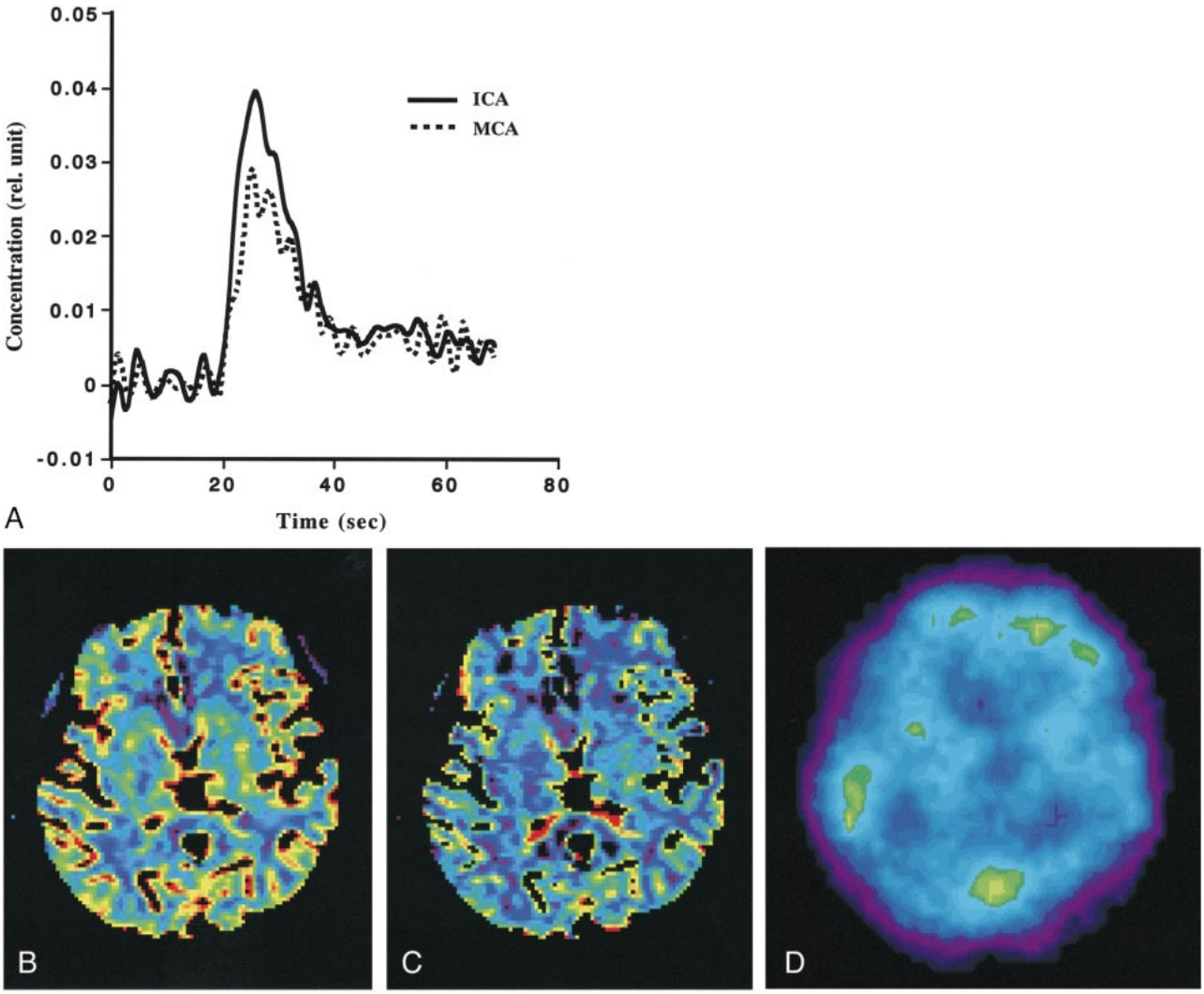

FIG 2. Example of PWI and ^{133}Xe-SPECT studies in patient 7.

A, Comparison of the AIFs obtained from the ICA and MCA. Note that they vary slightly and that the AIF from the ICA is somewhat better than that from the MCA.

B, rCBF image generated from PWI (rCBF-PWI).

C, rCBV image generated from PWI (rCBV-PWI).

D, ^{133}Xe-SPECT scan. Note that images generated from PWI were superior to ^{133}Xe-SPECT scan in spatial resolution, and that rCBF and rCBV values in the deep brain structure can be evaluated on rCBF-PWI and rCBV-PWI images.

ure 2B and C shows an example of the rCBF-PWI and rCBV-PWI scans from the same patient. The generated rCBF-PWI and rCBV-PWI studies were superior to the ^{133}Xe-SPECT study in spatial resolution, providing quantitative values (Fig 2B–D). The rCBF and rCBV values were also obtained by placing the ROI on the images. Using the rCBF-PWI and rCBV-PWI studies, we could evaluate deep brain structures, such as the basal ganglia, that are potentially difficult to evaluate by ^{133}Xe-SPECT owing to the low energy of xenon-133. Figure 3 shows the relationship between rCBF-PWI and rCBF-SPECT, for which we found a significant correlation ($r = .648$, n = 78; $P < .0001$).

In the region with severely decreased perfusion reserve, rCBF-SPECT was significantly lower than it was in the regions of moderately decreased or normal perfusion reserve ($P = .0005$ and $P < .0001$, respectively) (Fig 4A). Similarly, the regions with severely decreased perfusion reserve showed significantly lower rCBF-PWI than did the regions with moderately decreased or normal perfusion reserve ($P = .001$ and $P = .0004$, respectively) (Fig 4B). In contrast, significantly higher rCBV-PWI values were found in regions of severely decreased perfusion reserve relative to the values in regions of moderately decreased or normal perfusion reserve ($P = .006$ and $P = .022$, respectively) (Fig 4C). No significant differences in rCBF-SPECT, rCBF-PWI, and rCBV-PWI were found between regions of moderately decreased and normal perfusion reserve (Fig 4A–C).

Discussion

PWI, which shows the kinetics of a rapid bolus of paramagnetic contrast agent on serial T2*-

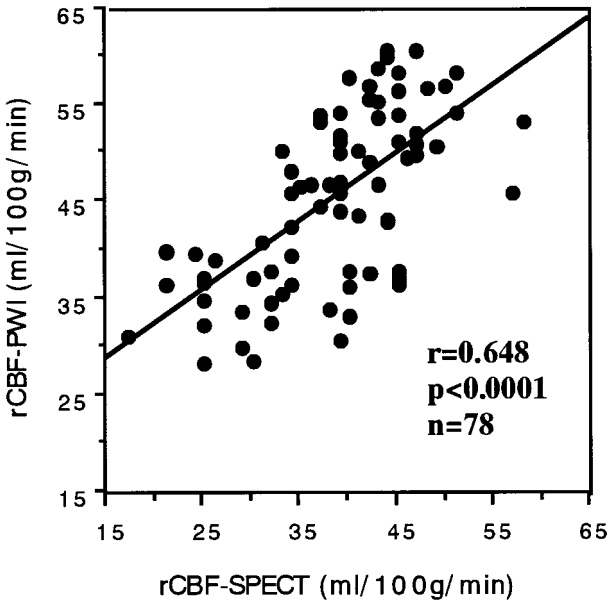

FIG 3. Relationship between the rCBF values obtained from ^{133}Xe-SPECT (rCBF-SPECT) and those obtained PWI (rCBF-PWI). A significant correlation was found between them (r = .648, $P < .0001$, n = 78).

weighted MR images, has been used to calculate rCBV and rCBF. In an early PWI study, single-slice dynamic susceptibility contrast-enhanced MR imaging with a gradient field-echo sequence was used, but this technique could not determine the AIF, since the ICA and MCA were not included in the slice imaged (33). Thus, PWI has been used only for estimating the relative values of rCBF and rCBV by calculating the area under the time-concentration curves. Although the relative values of hemodynamic parameters are informative for clinical use (20), quantification of rCBF and rCBV would be of greater value in making decisions for patient care. Recently, technical advances in MR equipment have enabled the use of multislice EPI sequences, making it possible to determine AIF from the ICA or MCA. In some studies, the AIF has been obtained from the ICA when PWI was performed using half-Fourier single-shot turbo spin-echo sequences (21), dual gradient-echo multishot EPI sequences (22), and dual fast low-angle shot sequences (23). It was also been reported that AIF has been obtained from the MCA by using the single-shot EPI sequence (25, 26, 34). To our knowledge, it has not been concluded which artery is more suitable for extraction of AIF.

We compared the AIFs obtained from the ICA and MCA, as shown in Figure 2A, and although we did not find a large difference between them, the AIF obtained from the ICA was, in general, somewhat better than that from the MCA. We therefore used the AIF from the ICA for deconvolution analysis in this study.

Because the gradient-echo sequence is sensitive to large vessels, the large vessels tend to appear prominently on the brain surface on the PWI studies obtained by using the standard procedure. Ernst et al (28) described a procedure for eliminating larger vessels by using a threshold determined simply by 2.5 times the median of all rCBF values. In this study, we tried to eliminate superficial vessels objectively by using the sophisticated automatic threshold selection method based on the procedure reported by Otsu (30). The rCBF-PWI and rCBV-PWI studies with elimination of superficial vessels were validated by visual analysis, allowing us to measure rCBF and rCBV without incurring contamination from superficial vessels.

There are some limitations to our method. Ostergaard et al (26) reported that the K value in Equations 3 and 4 was 1.09 for pigs and 0.87 for human volunteers (25) for absolute quantification of rCBF. In our study, however, we could not find the K value suitable for absolute quantification. Thus, instead of taking the K value constant, we calculated it by substituting 22 mL/100 g per minute for the CBF value in the white matter despite the presence of ischemia. One reason why we could not obtain a suitable K value may be that our subjects were older than those in the study by Ostergaard et al (26) and that they had occlusive carotic diseases. Another reason may be that the temporal resolution of our imaging sequence was inferior to that obtained by the previous investigators. Although our method might not be quantitative for these reasons, we believe that it is clinically useful, because the rCBF values we obtained correlated well with those from the ^{133}Xe-SPECT data (Fig 3). Additionally, we could not register the PWI and SPECT studies, since the spatial resolution of ^{133}Xe-SPECT scans is quite inferior to that of PWI images. Thus, a point-to-point correlation between rCBF and rCBV values was not carried out. The rCBF or rCBV value was calculated and evaluated for each ACA, ABZ, MCA, PBZ, and PCA territory. Because we evaluated each territory separately, we believe that the spatial difference did not influence our results.

Gadopentetate dimeglumine is not a diffusible tracer and cannot pass through the blood-brain barrier, unlike xenon-133. PWI is probably sensitive to the total blood component in the measured tissue, including that of the arterioles and venules (29). Although the principal of CBF measurement for PWI is different from that for xenon-133, and there are some limitations to our method, as described above, the rCBF values obtained with the two procedures were well correlated (Fig 3). The rCBF-PWI and rCBV-PWI studies, with quantitative values, were superior to the ^{133}Xe-SPECT scans in spatial resolution (Fig 2). The rCBF-PWI and rCBV-PWI studies could be used to evaluate hemodynamic changes, even in deep brain structures.

As shown in Figure 4, the regions with severely decreased perfusion reserve had significantly lower rCBF-SPECT and rCBF-PWI values and higher rCBV-PWI values than did the regions with mod-

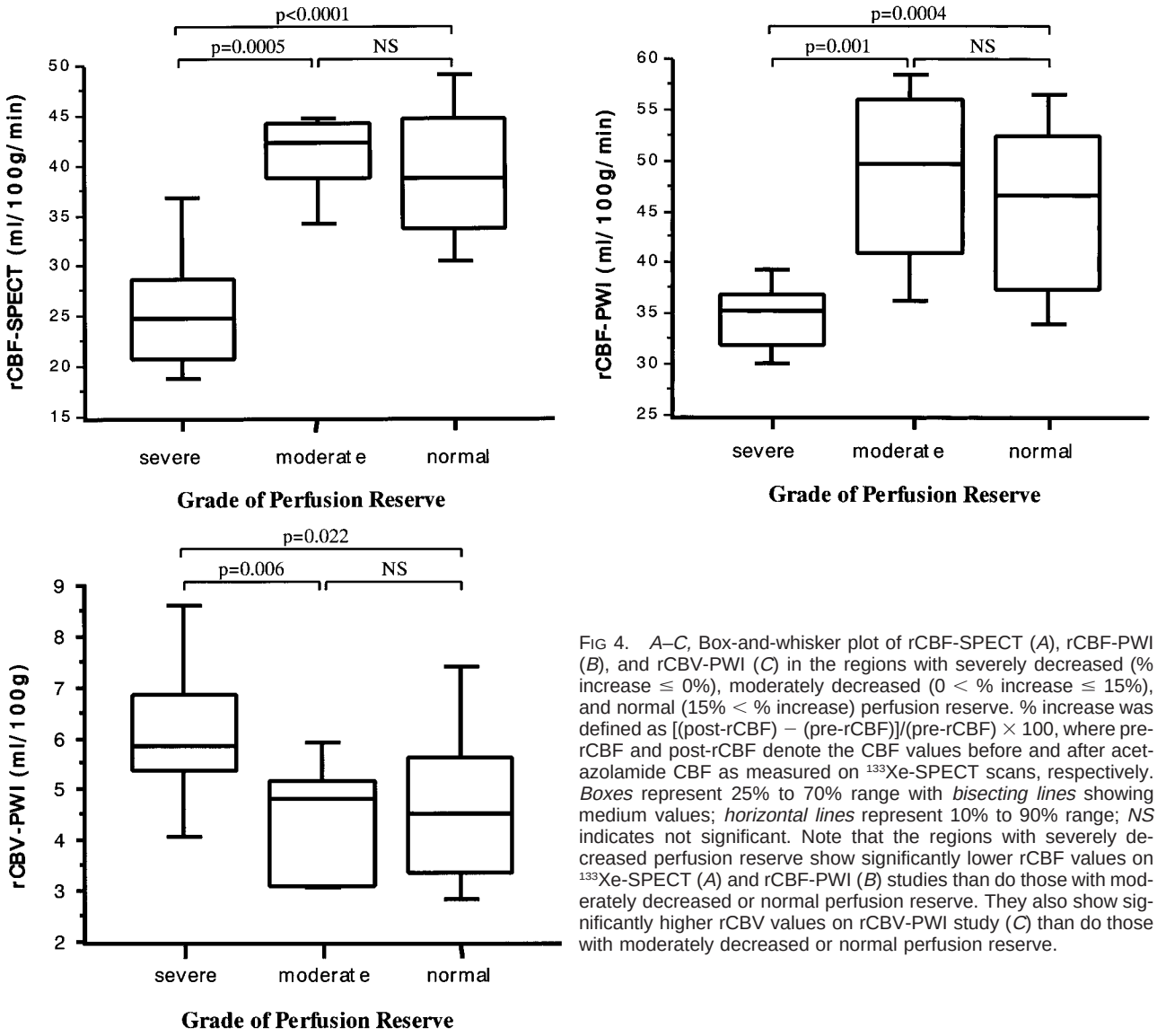

FIG 4. *A–C,* Box-and-whisker plot of rCBF-SPECT (*A*), rCBF-PWI (*B*), and rCBV-PWI (*C*) in the regions with severely decreased (% increase $\leq$ 0%), moderately decreased (0 $<$ % increase $\leq$ 15%), and normal (15% $<$ % increase) perfusion reserve. % increase was defined as [(post-rCBF) − (pre-rCBF)]/(pre-rCBF) × 100, where pre-rCBF and post-rCBF denote the CBF values before and after acetazolamide CBF as measured on ^{133}Xe-SPECT scans, respectively. *Boxes* represent 25% to 70% range with *bisecting lines* showing medium values; *horizontal lines* represent 10% to 90% range; *NS* indicates not significant. Note that the regions with severely decreased perfusion reserve show significantly lower rCBF values on ^{133}Xe-SPECT (*A*) and rCBF-PWI (*B*) studies than do those with moderately decreased or normal perfusion reserve. They also show significantly higher rCBV values on rCBV-PWI study (*C*) than do those with moderately decreased or normal perfusion reserve.

erately decreased or normal perfusion reserve. However, the number of patients included in this study may be too few to establish excellent statistical validation.

The high rCBV values found in the regions with severely decreased perfusion reserve were probably the result of maximal vasodilatation due to reduced cerebral perfusion pressure (CPP). These findings support the results obtained with PET studies (1–5). It is well known that when local CPP falls, cerebrovascular autoregulation occurs and precapillary resistance vessels dilate. This causes an increase in local CBV for maintaining local CBF. When compensatory vasodilatation is maximal, the autoregulation limit is reached, and a further decrease in local CPP will lead to a decrease in CBF. Additionally, the region in which a response against CO_2 disappeared showed an increased oxygen extraction rate (OER) in PET studies. The regions with decreased CBF and increased OER were reported as areas of misery perfusion and as good candidates for EC-IC bypass surgery. The phenomenon of a disappearing CO_2 response is comparable to that of a severely decreased acetazolamide response (% increase = 0%) in our study. Our results indicate that a combination of rCBF-PWI and rCBV-PWI can be used to depict the region with decreased CPP, and may suggest the area of misery perfusion. PWI may provide important clinical information for evaluating the degree of cerebral perfusion reserve impairment.

MR contrast agents are not radioactive and are relatively inexpensive as compared with tracers used in PET and SPECT studies. Furthermore, the additional scan time required to obtain PWI measurements is less than 2 minutes, and PWI can record rCBF and rCBV values simultaneously by a single acquisition without acetazolamide. PWI has some advantages over ^{133}Xe-SPECT in these respects when evaluating brain perfusion.

Conclusion

The multishot EPI sequence and automatic threshold selection procedure we used provides quantitative rCBF-PWI and rCBV-PWI studies from dynamic susceptibility contrast-enhanced MR images. The rCBF-PWI and rCBV-PWI studies generated simultaneously by our method appear to contribute clinically useful information for evaluating brain perfusion in patients with chronic ischemia.

References

1. Powers WJ, Raichle ME. **Positron emission tomography and its application to the study of cerebrovascular disease in man.** *Stroke* 1985;16:361–376
2. Gibbs JM, Leenders KL, Wise RJ, Jones T. **Evaluation of cerebral perfusion reserve in patients with carotid-artery occlusion.** *Lancet* 1984;1:182–186
3. Kuwabara Y, Ichiya Y, Sasaki M, et al. **PET evaluation of cerebral hemodynamics in occlusive cerebrovascular disease pre- and postsurgery.** *J Nucl Med* 1998;39:760–765
4. Baron JC, Bousser MG, Rey A, Guillard A, Comar D, Castaigne P. **Reversal of focal "misery-perfusion syndrome" by extra-intracranial arterial bypass in hemodynamic cerebral ischemia: a case study with ^{15}O positron emission tomography.** *Stroke* 1981;12:454–459
5. Kanno I, Uemura K, Higano S, et al. **Oxygen extraction fraction at maximally vasodilated tissue in the ischemic brain estimated from the regional CO2 responsiveness measured by positron emission tomography.** *J Cereb Blood Flow Metab* 1988;8:227–235
6. Frackowiak RS, Lenzi GL, Jones T, Heather JD. **Quantitative measurement of regional cerebral blood flow and oxygen metabolism in man using ^{15}O and positron emission tomography: theory, procedure, and normal values.** *J Comput Assist Tomogr* 1980;4:727–736
7. Yamaguchi T, Kanno I, Uemura K, et al. **Reduction in regional cerebral metabolic rate of oxygen during human aging.** *Stroke* 1986;17:1220–1228
8. Celsis P, Goldman T, Henriksen L, Lassen NA. **A method for calculating regional cerebral blood flow from emission computed tomography of inert gas concentrations.** *J Comput Assist Tomogr* 1981;5:641–645
9. Murase K, Tanada S, Inoue T, Ikezoe J. **Spectral analysis applied to dynamic single photon emission computed tomography studies with N-isopropyl-p-(123I)iodoamphetamine.** *Ann Nucl Med* 1998;12:109–114
10. Murase K, Tanada S, Fujita H, Sakaki S, Hamamoto K. **Kinetic behavior of technetium-99m-HMPAO in the human brain and quantification of cerebral blood flow using dynamic SPECT.** *J Nucl Med* 1992;33:135–143
11. Yonekura Y, Ishizu K, Okazawa H, et al. **Simplified quantification of regional cerebral blood flow with 99mTc-ECD SPECT and continuous arterial blood sampling.** *Ann Nucl Med* 1996; 10:177–183
12. Matsuda H, Higashi S, Kinuya K, et al. **SPECT evaluation of brain perfusion reserve by the acetazolamide test using Tc-99m HMPAO.** *Clin Nucl Med* 1991;16:572–579
13. Vorstrup S, Lassen NA, Henriksen L, et al. **CBF before and after extracranial-intracranial bypass surgery in patients with ischemic cerebrovascular disease studied with ^{133}Xe-inhalation tomography.** *Stroke* 1985;16:616–626
14. Vorstrup S, Brun B, Lassen NA. **Evaluation of the cerebral vasodilatory capacity by the acetazolamide test before EC-IC bypass surgery in patients with occlusion of the internal carotid artery.** *Stroke* 1986;17:1291–1298
15. Rosen BR, Belliveau JW, Vevea JM, Brady TJ. **Perfusion imaging with NMR contrast agents.** *Magn Reson Med* 1990;14: 249–265
16. Le Bihan D. **Magnetic resonance imaging of perfusion.** *Magn Reson Med* 1990;14:283–292
17. Le Bihan D. **Theoretical principles of perfusion imaging: application to magnetic resonance imaging.** *Invest Radiol* 1992; 27(Suppl 2):S6–S11
18. Karonen JO, Vanninen RL, Liu Y, et al. **Combined diffusion and perfusion MRI with correlation to single-photon emission CT in acute ischemic stroke: ischemic penumbra predicts infarct growth.** *Stroke* 1999;30:1583–1590
19. Sorensen AG, Copen WA, Ostergaard L, et al. **Hyperacute stroke: simultaneous measurement of relative cerebral blood volume, relative cerebral blood flow, and mean tissue transit time.** *Radiology* 1999;210:519–527
20. Hatazawa J, Shimosegawa E, Toyoshima H, et al. **Cerebral blood volume in acute brain infarction: a combined study with dynamic susceptibility contrast MRI and ^{99m}Tc-HMPAO-SPECT.** *Stroke* 1999;30:800–806
21. Koshimoto Y, Yamada H, Kimura H, et al. **Quantitative analysis of cerebral microvascular hemodynamics with T2-weighted dynamic MR imaging.** *J Magn Reson Imaging* 1999;9:462–467
22. Vonken EJ, van Osch MJ, Bakker CJ, Viergever MA. **Measurement of cerebral perfusion with dual-echo multi-slice quantitative dynamic susceptibility contrast MRI.** *J Magn Reson Imaging* 1999;10:109–117
23. Rempp KA, Brix G, Wenz F, Becker CR, Guckel F, Lorenz WJ. **Quantification of regional cerebral blood flow and volume with dynamic susceptibility contrast-enhanced MR imaging.** *Radiology* 1994;193:637–641
24. Ostergaard L, Weisskoff RM, Chesler DA, Gyldensted C, Rosen BR. **High resolution measurement of cerebral blood flow using intravascular tracer bolus passages, I: mathematical approach and statistical analysis.** *Magn Reson Med* 1996;36:715–725
25. Ostergaard L, Johannsen P, Host-Poulsen P, et al. **Cerebral blood flow measurements by magnetic resonance imaging bolus tracking: comparison with [(15)O]H_2O positron emission tomography in humans.** *J Cereb Blood Flow Metab* 1998;18:935–940
26. Ostergaard L, Smith DF, Vestergaard-Poulsen P, et al. **Absolute cerebral blood flow and blood volume measured by magnetic resonance imaging bolus tracking: comparison with positron emission tomography values.** *J Cereb Blood Flow Metab* 1998; 18:425–432
27. Murase K, Kikuchi K, Miki H, Shimizu T, Mochizuki T, Ikezoe J. **Determination of arterial input function using fuzzy c-means clustering for quantification of cerebral blood flow with dynamic susceptibility contrast-enhanced MR imaging.** In: *Book of Abstracts: 8th Annual Meeting of the International Society for Magnetic Resonance in Medicine.* International Society for Magnetic Resonance in Medicine; Berkely: 2000:471
28. Ernst T, Chang L, Itti L, Speck O. **Correlation of regional cerebral blood flow from perfusion MRI and spect in normal subjects.** *Magn Reson Imaging* 1999;17:349–354
29. Boxerman JL, Hamberg LM, Rosen BR, Weisskoff RM. **MR contrast due to intravascular magnetic susceptibility perturbations.** *Magn Reson Med* 1995;34:555–566
30. Otsu N. **A threshold selection method from gray-level histograms.** *IEEE Trans Syst Man Cybern* 1979;SMC-9:62–66
31. Kanno I, Lassen NA. **Two methods for calculating regional cerebral blood flow from emission computed tomography of inert gas concentrations.** *J Comput Assist Tomogr* 1979;3:71–76
32. Sugawara Y. **SPECT evaluation of cerebral perfusion reserve in patients with occlusive cerebrovascular diseases: evaluation with acetazolamide test and crossed cerebellar diaschisis.** *Kaku Igaku* 1995;32:287–299
33. Edelman RR, Mattle HP, Atkinson DJ, et al. **Cerebral blood flow: assessment with dynamic contrast-enhanced T2*-weighted MR imaging at 1.5 T.** *Radiology* 1990;176:211–220
34. Ostergaard L, Sorensen AG, Kwong KK, Weisskoff RM, Gyldensted C, Rosen BR. **High resolution measurement of cerebral blood flow using intravascular tracer bolus passages; II: experimental comparison and preliminary results.** *Magn Reson Med* 1996;36:726–736